

Structural Analysis of D-Phenylglycinamide Salts Uncovers Potential Pitfalls in Chiral Resolution via Diastereomeric Salt Formation

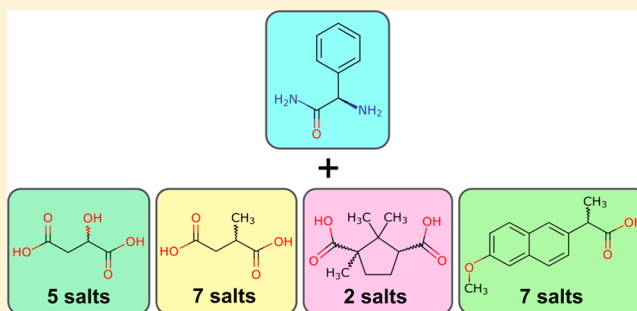
Natalia Tumanova,[†] Vanessa Seiler,[†] Nikolay Tumanov,[‡] Koen Robeyns,[†] Yaroslav Filinchuk,[†] Johan Wouters,[‡] and Tom Leyssens^{*,†}

[†]IMCN Institute of Condensed Matter and Nanosciences, Université catholique de Louvain, Place Louis Pasteur 1, 1348 Louvain-la-Neuve, Belgium

[‡]Chemistry Department, University of Namur, Rue de Bruxelles 61, 5000 Namur, Belgium

S Supporting Information

ABSTRACT: D-Phenylglycinamide (D-PGA) was shown to form diastereomeric salts with a series of dicarboxylic acids (malic, methylsuccinic, camphoric) and the drug naproxen. Structural analysis of the 21 newly discovered forms was performed in order to investigate the potential of D-PGA as a base agent for chiral resolution via diastereomeric salt formation. Malic and methylsuccinic dicarboxylic acids formed salts with 1:1 and 2:1 stoichiometries, whereas camphoric acid and naproxen yielded only 1:1 salts. In the D-PGA/naproxen system, variable-temperature in situ synchrotron X-ray diffraction gave access to two additional nonambient 1:1 salts. D-PGA subjected to liquid-assisted grinding with the racemic forms of the tested compounds to study chiral resolution in the solid state yielded in most of the cases complicated mixtures of diastereomeric salts or salts with the racemates (when both enantiomers and D-PGA crystallize in one structure), thereby suggesting that the use of D-PGA for chiral resolution may be challenging.



INTRODUCTION

For the majority of chiral drugs only one of the enantiomers exhibits the desired therapeutic effect, whereas harmful secondary effects can appear for the opposite optical isomer.¹ This is why many modern drugs are preferred to be enantiopure as it would allow a better control over the drug's performance in the body. Multiple chiral resolution techniques have been developed for this purpose,² with diastereomeric salt formation and chiral chromatography being the most extensively used in industry. There are also less widely applied alternative approaches, e.g., preferential crystallization,^{3,4} preferential enrichment,^{5,6} kinetic resolution,^{7,8} Viedma ripening,^{9–12} and chiral resolution based on cocrystallization.^{13–17}

While chiral chromatography is expensive as it requires chiral columns, diastereomeric salt formation offers a relatively cheap crystallization-based approach for chiral resolution.^{18–24} This technique implies selecting a certain chiral base/acid that would form diastereomeric salts with the target racemic compound. Diastereomeric salts may exhibit very distinct physical properties, for instance, solubility or density, relying on which they can be separated.²⁵ The acid/base used for salt formation can be removed after the separation step.

Enantiopure phenylglycinamide has been actively used as a chiral auxiliary in organic synthesis for diastereoselective reactions,^{26,27} as a key intermediate in the enzymatic synthesis of β -lactam antibiotics²⁸ and was also mentioned to be used as

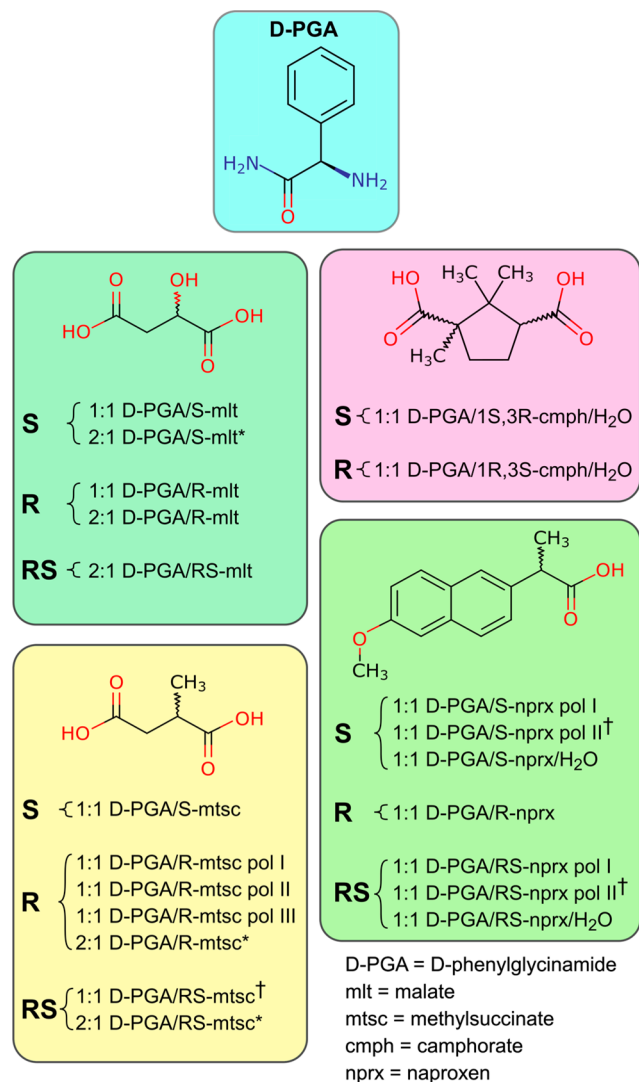
a base for chiral resolution of racemic mandelic acid via diastereomeric salt formation.²⁹ Despite a wide application of phenylglycinamide, the Cambridge Structural Database does not contain any phenylglycinamide-containing structures or the structure of phenylglycinamide itself.

In this study, we tested the ability of D-phenylglycinamide (D-PGA) to form diastereomeric salts with three dicarboxylic acids, methylsuccinic, malic, and camphoric (see Scheme 1), as well as naproxen, a nonsteroidal anti-inflammatory drug followed by their structural analysis. Three dicarboxylic acids were selected as model compounds due to their variety in structural complexity and a possibility to study the formation of not only 1:1 but also 2:1 (D-PGA/acid) salts, owing to two carboxylic groups for hydrogen bonding with D-PGA. Naproxen (nprx) was selected to test the D-PGA's potential of being applied for diastereomeric salt formation on a currently used drug. Moreover, selected systems also allowed studying other polymorphism- and chirality-related aspects of salt formation encountered when working with chiral/racemic compounds. This work shows that D-PGA readily forms diastereomeric salts with the aforementioned compounds and uncovers some pitfalls that can be encountered when D-PGA is intended for chiral resolution.

Received: November 27, 2018

Revised: May 12, 2019

Published: June 10, 2019

Scheme 1. All Salts Discovered in This Work^a

^aKey: (*) only unit cell parameters available; (†) high-temperature phases discovered upon heating in VT-PXRD experiments.

EXPERIMENTAL SECTION

Materials. Compounds were purchased from Sigma-Aldrich, and solvents (HPLC grade) were from VWR International and used without further purification.

Laboratory Liquid-Assisted Grinding (LAG) and Laboratory Powder X-ray Diffraction. The main method used to produce D-PGA salts was liquid-assisted grinding (LAG) in the presence of a number of solvents (i.e., ethanol, isopropanol, acetonitrile, and methanol) depending on the system. Initial compounds were ground in a 1:1 or 2:1 (D-PGA/coformer) molar ratio. Further detailed information on each experiment can be found in Tables S2.1, S3.1, S4.1, and S5.1. Around 100 mg of total reactant powder was put into 2 mL Eppendorf tubes, along with 10–20 μ L of solvent and 5–6 stainless steel 2 mm balls and subjected to grinding in a Retsch MM400 mixer mill for 60 or 90 min at a frequency of 30 Hz. The resulting powders were analyzed by laboratory powder X-ray diffraction (lab PXRD) using an X'pert PRO PANalytical diffractometer (2θ scanned from 2.5 to 40° with a step of 0.017°, CuK α radiation, Bragg–Brentano geometry). Collected diffraction powder data were analyzed and compared to the diffraction data of pure compounds using the FullProf Suite^{30,31} in order to establish formation of new phases.

Single-Crystal X-ray Diffraction Analysis. Single crystals suitable for X-ray diffraction analysis were obtained by slow evaporation. The crystal growth details are given in Table S1.1.

The structures were determined from single-crystal X-ray diffraction data collected using an Oxford Diffraction Gemini Ultra R diffractometer (CuK α radiation) or a MAR345 image plate detector using MoK α radiation (Rigaku UltraX 18S rotation anode, Xenocs Fox3D focusing multilayer mirror) in the case of D-PGA/R-nprx. The data were integrated using the CrysAlisPro³² software. The structures were solved by the dual-space algorithm implemented in SHELXT³³ and refined by full-matrix least-squares on $|F|^2$ using SHELXL-2014,³⁴ the shelXL³⁵ shell and Olex2 software.³⁶ Non-hydrogen atoms were refined anisotropically, and hydrogen atoms were located from the difference Fourier map but placed on calculated positions in riding mode with equivalent isotropic temperature factors fixed at 1.2 times U_{eq} of the parent atoms (1.5 times U_{eq} for methyl groups).

Disordered molecules were modeled appropriately. The 1:1 D-PGA/S-mtsc and 1:1 D-PGA/1S,3R-cmph/H₂O were remeasured at 110 and 100 K, respectively. D-PGA/1S,3R-cmph/H₂O exhibited an order–disorder phase transition with doubling of the c parameter and thus the unit cell volume (Figure S6.1).

The crystal data, data collection, and refinement details are summarized in Table S1.2.

Figures were generated using the Mercury program;³⁷ crystallographic information files were finalized using the Encifer³⁸ program.

Synchrotron Powder X-ray Diffraction and Variable-Temperature in Situ PXRD (VT-PXRD) Data Collection. Synchrotron PXRD data were collected at the MS-X04SA beamline at the Swiss-Norwegian beamline BM1A³⁹ at the European Synchrotron Radiation Facility (ESRF, Grenoble, France), using a PILATUS 2 M hybrid pixel detector at a wavelength of 0.6866 or 0.78487 Å. The wavelength was calibrated using a standard LaB₆ sample. Powder samples were packed into 0.5 mm glass capillaries, hand-ground beforehand to ensure better packing efficiency. Collected PXRD data were integrated using the SNBL toolbox program.³⁹

VT-PXRD was performed for selected samples obtained by LAG. Samples were heated at a rate of 5 °C/min. The diffraction patterns were collected simultaneously upon heating with the acquisition time for each frame being 20 s. The data from VT-PXRD experiments were treated using the Powder 3D software.⁴⁰

Structure Determination from PXRD. Five structures were determined from powder X-ray diffraction data: D-PGA/S-nprx pol I and pol II, D-PGA/RS-nprx pol I and pol II, and 1:1 D-PGA/RS-mtsc.

The initial model of the structure of D-PGA/S-nprx pol I was determined from PXRD data collected using an X'pert PRO PANalytical diffractometer (2θ scanned from 2.5 to 40° with a step of 0.017°) and further Rietveld refined using synchrotron X-ray data.

The structures of D-PGA/S-nprx pol II, D-PGA/RS-nprx pol I and pol II, as well as 1:1 D-PGA/RS-mtsc were solved from the data collected during VT-PXRD experiment.

Indexing and Le Bail fit were performed using the FOX program.⁴¹ The structures were found by global optimization in direct space (Monte Carlo/parallel tempering algorithm) using the FOX program⁴¹ and further refined by the Rietveld method in the TOPAS V5⁴² software (text based input files prepared in the jedit editor⁴³ were used). Profile parameters were found from Pawley refinement and then fixed in further Rietveld refinement cycles. The background was described manually using 20–25 points. In Rietveld refinement, molecules were described as rigid body objects, with only torsion angles, molecular position, and orientation refined. The equivalent isotropic temperature factors for hydrogen atoms were set at 1.2 times of those of parent atoms or 1.5 for methyl groups. The equivalent isotropic temperature factors for non-hydrogen atoms were refined with the maximum value set at 10.

From the found unit cell parameters, the volume of the asymmetric unit of the D-PGA/RS-nprx pol I suggested that R- and S-nprx occupy the same position. The diffraction pattern for this compound was similar to the one of the D-PGA/R-nprx. Thus, we used the initial D-PGA/R-nprx as a starting model for Rietveld refinement and introduced disorder to its –CH₃ and –H at the asymmetric carbon,

which corresponded to R- and S-enantiomers, respectively, fixing the occupancies at 0.5 (Figure S7.2). In the 1:1 D-PGA/RS-mtsc, R- and S-enantiomers of the acid also shared the same position; thus, the disorder was introduced in a similar manner (Figure S9.1).

The Rietveld refinement plots are given in Figures S1.4–S1.8. The crystal data, data collection, and refinement details are given in Table S1.2.

For 2:1 D-PGA/S-mlt, 2:1 D-PGA/R-mtsc, and 2:1 D-PGA/RS-mtsc only unit cell parameters were found from PXRD, which are listed in Table S1.3, with Pawley fitting plots given in Figures S1.1–S1.3.

RESULTS AND DISCUSSION

All four systems followed the procedure: (1) LAG in 1:1 and 2:1 ratios for D-PGA and enantiopure S- and R-dicarboxylic acids (methylsuccinic, malic, and camphoric) and in 1:1 ratio for R- and S-nprx in order to identify the possibility of salt formation; (2) crystallization from solution to obtain single crystals suitable for X-ray diffraction analysis; (3) LAG of D-PGA with the racemic forms of the dicarboxylic acids and nprx in order to verify the possibility of chiral resolution in the solid state. Moreover, the powder diffraction patterns of selected samples were remeasured using synchrotron radiation to get data with better resolution enabling structure determination for the salts when no single crystals were produced. Below, we present and discuss the results first for dicarboxylic acids and then separately for nprx, followed by general conclusions.

D-PGA/Dicarboxylic Acids. D-PGA/malic acid yielded five salts: 1:1 D-PGA/S-mlt, 2:1 D-PGA/S-mlt, 1:1 D-PGA/R-mlt, 2:1 D-PGA/R-mlt, and 2:1 D-PGA/RS-mlt (Scheme 1). Each combination of enantiomers yielded salts with two stoichiometries, 1:1 and 2:1, owing to two binding sites via the carboxyl groups (see Table S2.1). Several of the 1:1 powders obtained by LAG often contained some residual amounts of the 2:1 phase, suggesting that the 1:1 salt might form through an intermediate 2:1 salt. It is known from the literature that the formation of some 1:1 salts (or cocrystals) goes through an intermediate 2:1 phase.^{44–47} We tested if this was the case for D-PGA/malates. A step-by-step grinding experiment—wherein the first step LAG is performed in the 2:1 ratio in order to obtain the 2:1 salt and in the second step, another equivalent of acid is added to the produced salt—suggested that this mechanism is plausible as the second step resulted in 1:1 D-PGA/malates for both R- and S-enantiomers of malic acid (see samples 17 and 18 in Table S2.1).

Methylsuccinic acid is structurally similar to malic acid, except that the hydroxyl group is changed for a methyl group. In the D-PGA/methylsuccinic acid system, we found seven salts: 1:1 D-PGA/S-mtsc, three polymorphs of 1:1 D-PGA/R-mtsc, 2:1 D-PGA/R-mtsc, 2:1 D-PGA/RS-mtsc and 1:1 D-PGA/RS-mtsc (Scheme 1).

The combination with R-methylsuccinic acid turned out to be much richer in forms than D-PGA/S-methylsuccinic acid, which yielded only one salt (Scheme 1). This finding highlights that chirality, and, in other words, the three-dimensional structure of both salt formers matters and is most likely behind a rich variety of forms in the case of R-methylsuccinic acid in comparison with S-methylsuccinic acid as hydrogen-bonding sites stay the same for both acids.

From the LAG experiments (Table S3.1), we did not find any consistent conditions for the formation of any particular 1:1 D-PGA/R-mtsc polymorph. They seemed to have equal probabilities to emerge and sometimes as mixtures, no matter which solvent was used, thus indicating that the phases compete kinetically. The reaction outcome may also depend

on the duration of grinding as we often consistently obtained 1:1 D-PGA/R-mtsc pol I, when the reaction was performed for 90 min (samples 7, 9, and 11 in Table S3.1), whereas the result was less predictive for reaction times of 60 min. Polymorphic transitions can be induced by mechanochemical treatment, which is why the duration of grinding is important as some forms can withstand grinding, while others may emerge and disappear in the course of reaction.^{48–50} Stopping the reaction at a particular moment can thus lead to obtaining various forms.

Similarly to the D-PGA/malic acid system, a two-step mechanism was suspected for the 1:1 D-PGA/R-mtsc via an intermediate 2:1 D-PGA/R-mtsc phase. After the second step, we obtained the 1:1 D-PGA/R-mtsc pol I salt in the case of 90 min methanol-assisted grinding (sample 22 in Table S3.1), whereas 60 min isopropanol-assisted grinding led to a mixture of all three 1:1 D-PGA/R-mtsc polymorphs (sample 23 in Table S3.1). Such a result shows that polymorph I can be a thermodynamically stable form, whereas the other two polymorphs are metastable and disappear if grinding is performed for an extended time. This is in agreement with the experiments described above, according to which we often observed polymorph I after 90 min LAG reaction, whereas shorter reactions led to polymorph mixtures. The reaction outcome can also be solvent dependent, as it may affect the reaction rate and thus interconversion of polymorphs.^{44,50}

Camphoric acid represents a more structurally complex compound as it occupies a larger volume due to a five-membered ring. The D-PGA/camphoric acid system yielded only two hydrated salts: 1:1 D-PGA/1R,3S-cmph/H₂O and 1:1 D-PGA/1S,3R-cmph/H₂O (Scheme 1 and Table S4.1). We suggest that the structure easily incorporates water, probably from air during grinding or due to a residual amount of water in solvents. All our attempts to obtain nonhydrated salts failed.

When D-PGA was subjected to LAG with the racemic forms of the initial dicarboxylic acids, the resultant powders turned out to be mixtures of multiple phases. LAG reactions with compounds taken in the 1:1 ratio led to mixtures of the corresponding 1:1 diastereomeric salts (samples 13 and 14 in Table S2.1; 18 and 19 in Table S3.1; 12 and 13 in Table S4.1), whereas 2:1 reactions performed for malic and methylsuccinic acids yielded mainly 2:1 salts containing both enantiomers of the acid (D-RS salts, samples 15 and 16 in Table S2.1; 20 and 21 in Table S3.1), thus demonstrating chiral resolution in the first mentioned case but not in the second. Moreover, when a sample obtained by 1:1 LAG of D-PGA with RS-methylsuccinic acid (sample 18 in Table S3.1) was heated in a capillary, another phase was revealed. This phase emerged around 145 °C when the initial mixture of diastereomeric salts started to disappear (Figure S3.10). This new phase was determined from powder X-ray diffraction to be a 1:1 salt of D-PGA and RS-methylsuccinic acid. Since this phase was not observed at room temperature, we suggest that higher temperatures allow greater disorder opportunities for methylsuccinic acid, enabling R- and S-enantiomers to occupy the same position (Figure S9.1).

Structural Analysis. In general, all the 1:1 salts formed by D-PGA and the dicarboxylic acids exhibit structures composed of alternating layers formed by the carboxylate anions and positively charged D-PGA molecules. However, bonding between the molecules within a layer or between adjacent layers slightly varies. Figure 1 demonstrates the structural features of the 1:1 D-PGA salts with dicarboxylic acids.

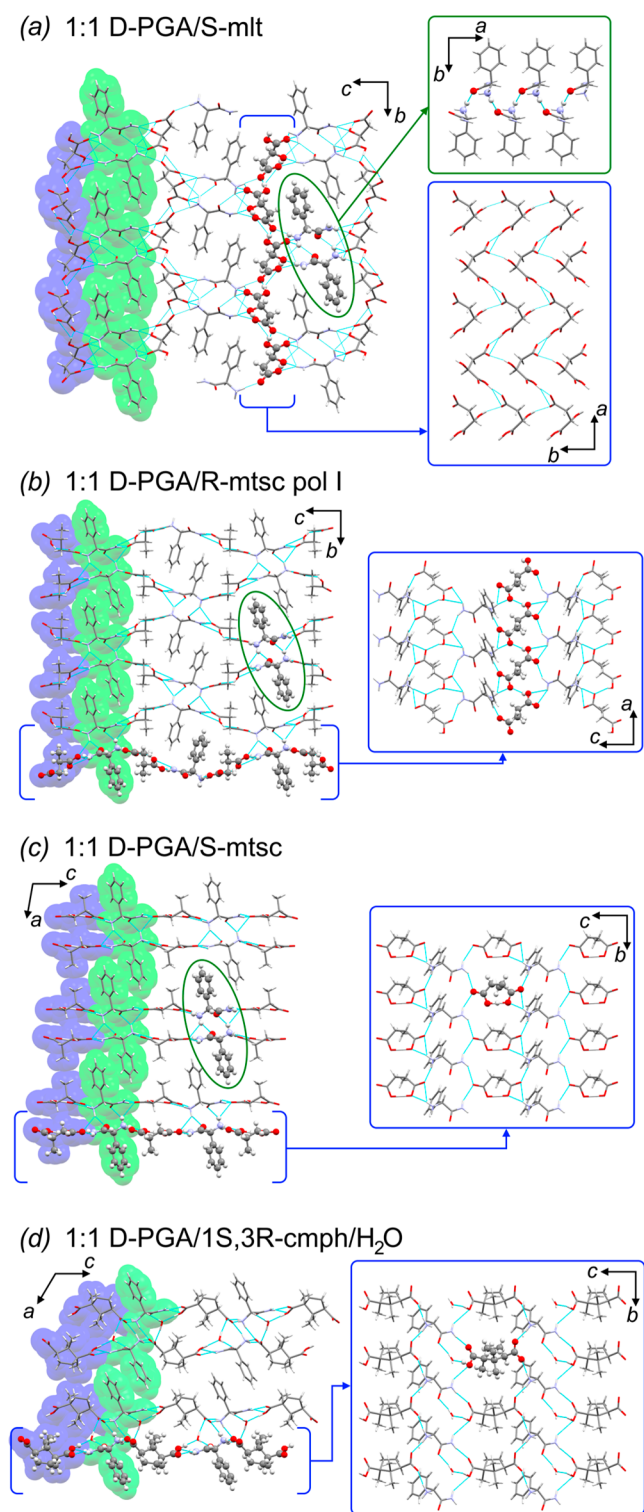


Figure 1. Structural representation of selected 1:1 D-PGA salts formed with the studied dicarboxylic acids. Green ellipses highlight D-PGA chains formed in the same manner in all other presented structures as shown in (a). Structural fragments enclosed in blue rectangles on the right show a motif highlighted with ball-and-stick style and taken in brackets in the left figure. Space-fill style indicates alternating layers formed by acid (blue) and D-PGA (green). Ball-and-stick style in the left panels highlights either a chain as in (b) or not interconnected semi-deprotonated acid as in (c) and (d).

Positively charged D-PGA tended to form infinite chains along one of the axes via N–H···O hydrogen bonding between

its ammonium group and oxygen of the amide group (Figure 1a–c), except for the hydrated cmph salts, in which oxygen of the amide group was instead engaged in hydrogen bonding with water molecules (Figure 1d).

Carboxylate layers were either formed by molecules interconnected into sheets, as in 1:1 D-PGA/S-mlt (Figure 1a) and 1:1 D-PGA/R-mlt, by molecules forming infinite chains as in 1:1 D-PGA/R-mtsc pol I (Figure 1b) and II, or by simply individual molecules as in 1:1 D-PGA/S-mtsc (Figure 1d) and 1:1 D-PGA/R-mtsc pol III. The reason why in the last two cases acid molecules were not interconnected is because the hydrogen of the carboxyl group formed an intramolecular O–H···O hydrogen bond with the carboxylate and thus was prevented from forming any other hydrogen bonds.

A strong intramolecular O–H···O hydrogen bond formed between the carboxylate and carboxyl groups of mtsc anions, as for instance in 1:1 D-PGA/S-mtsc, might also hinder deprotonation of the second carboxyl group, thereby preventing formation of a 2:1 salt, whose analogue was observed for the D-PGA/R-methylsuccinic acid combination.

Formation of sheets of interconnected mlt anions in 1:1 D-PGA/S-mlt and D-PGA/R-mlt became possible owing to the hydroxyl group offering an additional site for hydrogen bonding. In the camphorates, the carboxylates were not interconnected as the carboxyl group was instead engaged in hydrogen bonding with water. Connection between the D-PGA and carboxylate layers was provided via N–H···O hydrogen bonding.

The diffraction patterns of the 1:1 D-PGA/S-mlt and D-PGA/R-mlt are hardly different due to their highly similar structures (Figure S8.1). The structures of the 2:1 D-PGA/R-mlt and 2:1 D-PGA/RS-mlt, being hardly distinguishable from each other (Figure S8.2), are different from those of the 1:1 salts. They are comprised of double sheets perpendicular to the *b* axis, with only weak interactions between the adjacent sheets arranged in a zip-like manner. Within a sheet, each mlt anion forms N–H···O hydrogen bonds with six positively charged D-PGA molecules and at the same time connects two D-PGA molecules from the adjacent sheet. D-PGA molecules within a sheet form dimers, owing to N–H···O bonding.

Unfortunately, we were not able to obtain the structures of the 2:1 D-PGA/S-mlt, 2:1 D-PGA/R-mtsc, and 2:1 D-PGA/RS-mtsc salts—only the unit cell parameters were found to confirm the 2:1 stoichiometry (see Table S1.3). Our attempts to find the structure from synchrotron powder X-ray diffraction data failed as well. The found triclinic space group and unit cell volume suggested six molecules in the asymmetric unit cell for all three structures: four D-PGAs and two mlt or mtsc. The presence of six molecules in the asymmetric unit for both salts rendered structure determination from PXRD extremely difficult.

D-PGA/Naproxen. D-PGA/nprx system yielded multiple salts of 1:1 stoichiometry: D-PGA/R-nprx, D-PGA/S-nprx pol I and II, D-PGA/S-nprx/H₂O, D-PGA/RS-nprx pol I and II, and D-PGA/RS-nprx/H₂O (Scheme 1). LAG experiments performed for this system are summarized in Table S5.1. D-PGA formed an unhydrated salt with R-nprx, whereas it tended to form a hydrated salt with S-nprx. To obtain the unhydrated form of D-PGA and S-nprx, we heated a sample obtained by acetonitrile-assisted grinding, which contained both the hydrated and unhydrated salts, simultaneously collecting powder synchrotron X-ray diffraction data. This was done assuming that the hydrated salt will disappear first upon

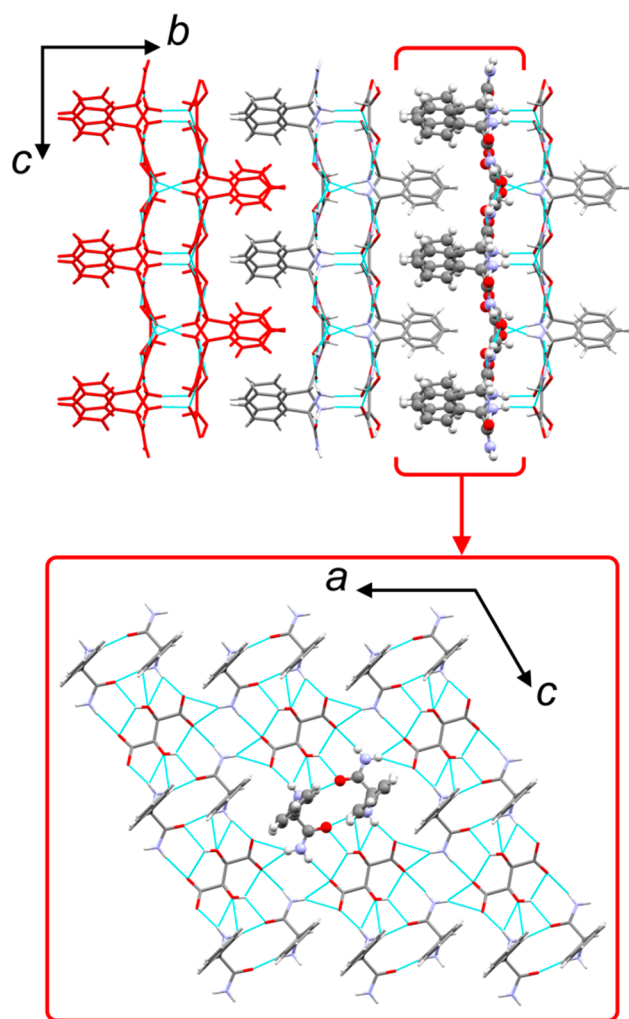


Figure 2. Structural representation of the 2:1 D-PGA/d-mlt salt. On the right image, one of the double sheets is highlighted in red; ball-and-stick style demonstrates one part of a double sheet, shown below in the *ac* projection.

heating due to water evaporation from its structure, thus giving access to the diffraction pattern of the pure unhydrated form. However, during heating, we observed another phase emerging when the initial two phases disappeared (Figure 3a). This phase was determined to be another polymorph of the unhydrated 1:1 salt (pol II).

In order to test the possibility of chiral resolution in the solid state, we performed several LAG experiments, which yielded powders containing both hydrated and unhydrated phases (samples 8–10 in Table S5.1). Acetonitrile-assisted grinding yielded mainly D-PGA/RS-nprx pol I salt and a very small amount of the hydrated phase present as impurity (sample 10 in Table S5.1). Upon heating this sample, we observed behavior similar to the D-PGA/S-nprx salt (Figure 3b), i.e., emergence of another polymorph of D-PGA/RS-nprx (pol II) with a structure similar to D-PGA/S-nprx pol II (Figure S7.5).

The D-PGA/RS-nprx/H₂O salt was almost isostructural to the D-PGA/S-nprx/H₂O, except that *R*- and *S*-nprx shared the same position in the former (Figures S7.1 and S7.3a). Moreover, the D-PGA/RS-nprx pol I salt turned out to be isostructural to D-PGA/R-nprx (Figures S7.2 and S7.4a), with again *R*- and *S*-nprx enantiomers occupying the same position. Because of the isostructurality observed in these two pairs of

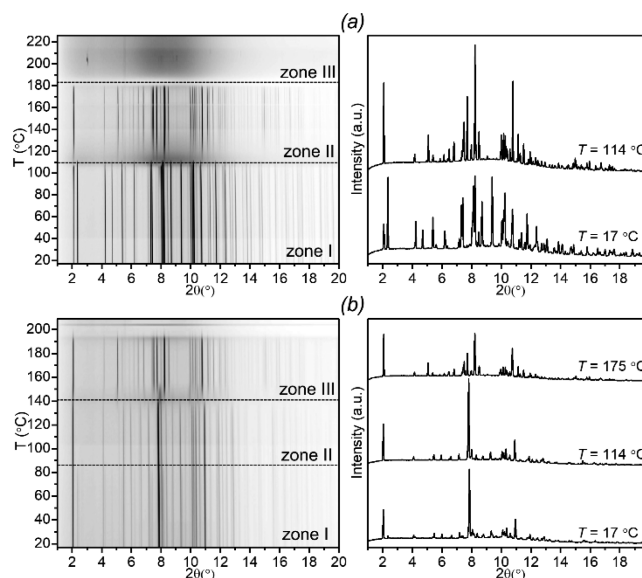


Figure 3. Powder X-ray diffraction patterns collected upon heating for (a) the D-PGA/S-nprx (sample #2 in Table S5.1) and (b) the D-PGA/RS-nprx (sample #10 in Table S5.1) samples, both obtained by 1:1 acetonitrile-assisted grinding. In (a), zone I ($T = 17\text{ }^{\circ}\text{C}$) – D-PGA/S-nprx/H₂O and D-PGA/S-nprx pol I; zone II ($T = 114\text{ }^{\circ}\text{C}$) – D-PGA/S-nprx pol II; and zone III – unknown phase (probably a chemical reaction as it emerges from melt). In (b), zone I ($T = 17\text{ }^{\circ}\text{C}$) – D-PGA/RS-nprx pol I and D-PGA/RS-nprx/H₂O; zone II ($T = 114\text{ }^{\circ}\text{C}$) – D-PGA/RS-nprx pol I; zone III ($T = 175\text{ }^{\circ}\text{C}$) – D-PGA/RS-nprx pol II.

salts, the diffraction patterns of the salts within a pair were hardly distinguishable (Figures S7.3b and S7.4b) and could have been easily confused with each other. The same phenomenon, when two nprx enantiomers shared the same position, was observed in nprx/proline (CCDC QIMBOG)⁵⁰ and nprx/piperazine (CCDC TOBMEE⁵¹) cocrystals, and several other naproxen-based compounds (CCDC DEVSIH,⁵² NALFEL,⁵³ and PEHXAE⁵⁴). These examples highlight the fact that even if a diffraction pattern looks like the one from the diastereomeric salt (or cocrystal), it can still be a salt (or cocrystal) with a racemic compound. Hence, such systems should be treated with caution when dealing with chiral resolution, and additional analyses besides X-ray diffraction should always be performed in order to distinguish diastereomeric salts from a simply isostructural salt with the racemate.

From the structural point of view, hydrated and unhydrated salts exhibit the same general packing: the structures are made of structural blocks; within a block, D-PGA and nprx are situated in a chess-like manner. These blocks are shifted one relative to the other along the *b* axis so that molecules of D-PGA and nprx from adjacent blocks are again arranged chess-like. In the unhydrated salts, the orientation of nprx molecules allows for a zip-like arrangement when considering two adjacent blocks. Figure 4 demonstrates the structures of D-PGA/S-nprx/H₂O and D-PGA/R-nprx as examples of hydrated and unhydrated salts. Each nprx molecule in all analyzed structures attaches D-PGA molecules via charge-assisted N–H···O hydrogen bonds, with the amine and amide groups of D-PGA and negatively charged carboxylate of nprx being involved. In the unhydrated salts, D-PGA molecules are connected directly one to another via N–H···O hydrogen

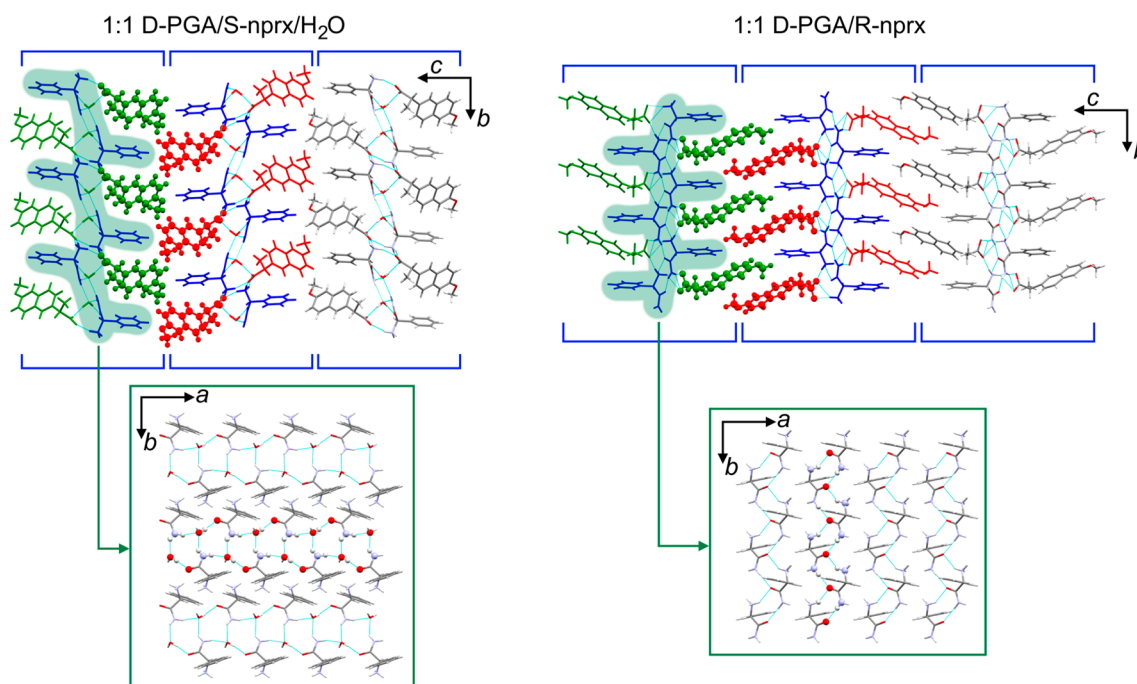


Figure 4. Structures of D-PGA/S-nprx/H₂O and D-PGA/R-nprx. The structures are made of structural blocks (enclosed in blue brackets). One of the D-PGA sheets in each structure is shadowed green and shown in a green rectangle in the *ab* projection below. Nprx molecules from two adjacent blocks are colored red and green.

bonds, whereas in the hydrated salts, D-PGA molecules are linked through water molecules. As follows from our experiments, the D-PGA/S-nprx and D-PGA/RS-nprx combinations incorporate water into their structure more easily than D-PGA/R-nprx, thus demonstrating that the final structure depends not only on the potential hydrogen-bonding sites but also on the three-dimensional suitability of both salt formers, which may facilitate or hinder water incorporation.

CONCLUSIONS

D-PGA readily forms diastereomeric salts with tested dicarboxylic acids and nprx. Malic and methylsuccinic acids yield not only 1:1 salts, but also those with the 2:1 stoichiometry. We suspect that the 2:1 phase is an intermediate and precedes the formation of the 1:1 phase. A better insight into a mechanism of this reaction can be obtained in situ ball-milling experiments taking into account that solid-state reactions may depend on multiple other factors, for instance, the degree of homogeneity during grinding or possible amorphization of reaction products^{44,55,56} (beyond the scope of the current paper).

The results of this work show that chirality plays a key role in the reaction outcome as enantiomers differ only by their three-dimensional arrangement of atoms, with all their functional groups prone to hydrogen bonding being the same. For instance, the D-PGA/S-nprx pair yielded a hydrate, whereas the D-PGA/R-nprx formed an unhydrated salt under the same conditions, thus suggesting that in the first case, water is more easily incorporated into the structure than in the second case. Another example is methylsuccinic acid: D-PGA formed three polymorphs of the 1:1 salt and one 2:1 salt with the R-enantiomer, whereas with the S-enantiomer, only a 1:1 salt. Such aspects of chirality have been already noted for cocrystallization reactions, when chirality not only affected the number of total forms obtained, but also led to enantiospecific

systems, in which only one of the enantiomers formed a cocrystal, but not the other.^{44,50,57}

Structural analysis of D-PGA salts showed that, despite the ability of D-PGA to readily form diastereomeric salts, its application for chiral resolution process could be challenging. For instance, the malic acid case demonstrates that obtained diastereomeric salts might be hardly distinguishable from a structural point of view, and, thus, have very similar physicochemical properties hindering their separation. The case of methylsuccinic acid shows that one of the enantiomers has an increased tendency to form polymorphs than the other. This may as well complicate a potential chiral resolution process. Finally, the cases of naproxen, malic acid, and methylsuccinic acid reveal the possible formation of a salt with the racemic form of a target compound, which should not be underestimated. Being aware of these potential pitfalls may help develop more robust and effective chiral resolution procedures based on diastereomeric salt formation not only for the D-PGA case but also for other potential diastereomeric salt forming agents.

ASSOCIATED CONTENT

Supporting Information

The Supporting Information is available free of charge on the ACS Publications website at DOI: 10.1021/acs.cgd.8b01769.

Additional details of experimental procedures, PXRD patterns and analysis, and additional structural figures (PDF)

Accession Codes

CCDC 1879650–1879670 contain the supplementary crystallographic data for this paper. These data can be obtained free of charge via www.ccdc.cam.ac.uk/data_request/cif, or by emailing data_request@ccdc.cam.ac.uk, or by contacting The

Cambridge Crystallographic Data Centre, 12 Union Road, Cambridge CB2 1EZ, UK; fax: +44 1223 336033.

AUTHOR INFORMATION

Corresponding Author

*E-mail: tom.leysens@uclouvain.be.

ORCID

Natalia Tumanova: 0000-0001-9762-9259

Nikolay Tumanov: 0000-0001-6898-9036

Yaroslav Filinchuk: 0000-0002-6146-3696

Author Contributions

The manuscript was written through contributions of all authors. All authors have given approval to the final version of the manuscript.

Notes

The authors declare no competing financial interest.

ACKNOWLEDGMENTS

The authors thank Université catholique de Louvain and FNRS (FRIA scholarship allocated to N.T.) for financial support, the Swiss-Norwegian beamline BM1A at the European Synchrotron Radiation Facility (ESRF, Grenoble, France) for the beam time allocation, and the PC² platform of the University of Namur for single-crystal and powder X-ray diffraction analyses.

ABBREVIATIONS

cmph, camphorate; D-PGA, D-phenylglycinamide; LAG, liquid-assisted grinding; mlt, malate; mtsc, methylsuccinate; nprx, naproxen; PXRd, powder X-ray diffraction; VT-PXRd, variable-temperature powder X-ray diffraction

REFERENCES

- (1) Nguyen, L. A.; He, H.; Pham-Huy, C. Chiral Drugs: An Overview. *Int. J. Biomed. Sci.* **2006**, *2*, 85–100.
- (2) *Enantiomer Separation: Fundamentals and Practical Methods*; Toda, F., Ed.; Springer: Netherlands, 2004; <https://doi.org/10.1007/978-1-4020-2337-8>.
- (3) Coquerel, G. Preferential Crystallization. *Top. Curr. Chem.* **2006**, *269*, 1–51.
- (4) Levilain, G.; Coquerel, G. Pitfalls and Rewards of Preferential Crystallization. *CrystEngComm* **2010**, *12*, 1983–1992.
- (5) Gonnade, R. G.; Iwama, S.; Mori, Y.; Takahashi, H.; Tsue, H.; Tamura, R. Observation of Efficient Preferential Enrichment Phenomenon for a Cocrystal of (DL)-Phenylalanine and Fumaric Acid under Nonequilibrium Crystallization Conditions. *Cryst. Growth Des.* **2011**, *11*, 607–615.
- (6) Iwama, S.; Kuyama, K.; Mori, Y.; Manoj, K.; Gonnade, R. G.; Suzuki, K.; Hughes, C. E.; Williams, P. A.; Harris, K. D. M.; Veessler, S.; Takahashi, H.; Tsue, H.; Tamura, R. Highly Efficient Chiral Resolution of DL-Arginine by Cocrystal Formation Followed by Recrystallization under Preferential-Enrichment Conditions. *Chem. - Eur. J.* **2014**, *20*, 10343–10350.
- (7) Métro, T.; Salom-Roig, X. J.; Reverte, M.; Martinez, J.; Lamaty, F. Faster and Cleaner Dynamic Kinetic Resolution via Mechanochemistry. *Green Chem.* **2015**, *17*, 204–208.
- (8) Schichl, D. a.; Enthaler, S.; Holla, W.; Riermeier, T.; Kragl, U.; Beller, M. Dynamic Kinetic Resolution of α -Amino Acid Esters in the Presence of Aldehydes. *Eur. J. Org. Chem.* **2008**, *2008*, 3506–3512.
- (9) Iggland, M.; Mazzotti, M. A Population Balance Model for Chiral Resolution via Viedma Ripening. *Cryst. Growth Des.* **2011**, *11*, 4611–4622.
- (10) Spix, L.; Meekes, H.; Blaauw, R. H.; van Enckevort, W. J. P.; Vlieg, E. Complete Deracemization of Proteinogenic Glutamic Acid

Using Viedma Ripening on a Metastable Conglomerate. *Cryst. Growth Des.* **2012**, *12*, 5796–5799.

(11) Viedma, C. Chiral Symmetry Breaking During Crystallization: Complete Chiral Purity Induced by Nonlinear Autocatalysis and Recycling. *Phys. Rev. Lett.* **2005**, *94*, 065504.

(12) Steendam, R. R. E.; Harmsen, B.; Meekes, H.; Van Enckevort, W. J. P.; Kaptein, B.; Kellogg, R. M.; Raap, J.; Rutjes, F. P. J. T.; Vlieg, E. Controlling the Effect of Chiral Impurities on Viedma Ripening. *Cryst. Growth Des.* **2013**, *13*, 4776–4780.

(13) Springuel, G.; Collard, L.; Leysens, T. Ternary and Quaternary Phase Diagrams: Key Tools for Chiral Resolution through Solution Cocrystallization. *CrystEngComm* **2013**, *15*, 7951–7958.

(14) Harmsen, B.; Leysens, T. Dual-Drug Chiral Resolution: Enantiospecific Cocrystallization of (S)-Ibuprofen Using Levetiracetam. *Cryst. Growth Des.* **2018**, *18*, 441–448.

(15) Harmsen, B.; Leysens, T. Enabling Enantiopurity: Combining Racemization and Dual-Drug Co-Crystal Resolution. *Cryst. Growth Des.* **2018**, *18*, 3654–3660.

(16) Springuel, G.; Leysens, T. Innovative Chiral Resolution Using Enantiospecific Co-Crystallization in Solution. *Cryst. Growth Des.* **2012**, *12*, 3374–3378.

(17) He, L.; Liang, Z.; Yu, G.; Li, X.; Chen, X.; Zhou, Z.; Ren, Z. Green and Efficient Resolution of Racemic Ofloxacin Using Tartaric Acid Derivatives via Forming Cocrystal in Aqueous Solution. *Cryst. Growth Des.* **2018**, *18*, 5008–5020.

(18) da Silva, C. C.; Martins, F. T. The Enantiopreference in the Solid State Probed in Lamivudine Crystal Forms with Mandelic Acid. *RSC Adv.* **2015**, *5*, 20486–20490.

(19) Nyhlén, J.; Eriksson, L.; Bäckvall, J.-E. Synthesis and Optical Resolution of an Allenic Acid by Diastereomeric Salt Formation Induced by Chiral Alkaloids. *Chirality* **2008**, *20*, 47–50.

(20) Martín, A.; Cocero, M. J. Separation of Enantiomers by Diastereomeric Salt Formation and Precipitation in Supercritical Carbon Dioxide. *J. Supercrit. Fluids* **2007**, *40*, 67–73.

(21) Simon, M.; Donnellan, P.; Glennon, B.; Jones, R. C. Resolution via Diastereomeric Salt Crystallization of Ibuprofen Lysine: Ternary Phase Diagram Studies. *Chem. Eng. Technol.* **2018**, *41*, 921–927.

(22) Lörcincz, L.; Bánsághi, G.; Zsember, M.; de Simón Brezmes, S.; Szilágyi, I. M.; Madarász, J.; Sohajda, T.; Székely, E. Diastereomeric Salt Precipitation Based Resolution of Ibuprofen by Gas Antisolvent Method. *J. Supercrit. Fluids* **2016**, *118*, 48–53.

(23) Kodama, K.; Nagata, J.; Kurozumi, N.; Shitara, H.; Hirose, T. Solvent-Induced Chirality Switching in the Enantioseparation of Regioisomeric Hydroxyphenylpropionic Acids via Diastereomeric Salt Formation with (1R, 2S)-2-Amino-1,2-Diphenylethanol. *Tetrahedron: Asymmetry* **2017**, *28*, 460–466.

(24) Wu, H.; West, A. R.; Vickers, M.; Apperley, D. C.; Jones, A. G. Synthesis, Crystallization and Characterization of Diastereomeric Salts Formed by Ephedrine and Malic Acid in Water. *Chem. Eng. Sci.* **2012**, *77*, 47–56.

(25) Pálovics, E.; Zsolt, S.; Beáta, S.; Miklós, B.; Elemér, F. Separation of Chiral Compounds: Enantiomeric and Diastereomeric Mixtures Diastereomeric Mixtures Emese. In *Laboratory Unit Operations and Experimental Methods in Chemical Engineering* **2018**, 99–122.

(26) Boesten, W. H. J.; Seerden, J. G.; de Lange, B.; Dielemans, H. J. A.; Elsenberg, H. L. M.; Kaptein, B.; Moody, H. M.; Kellogg, R. M.; Broxterman, Q. B. Asymmetric Strecker Synthesis of α -Amino Acids via a Crystallization-Induced Asymmetric Transformation Using (R)-Phenylglycine Amide as Chiral Auxiliary. *Org. Lett.* **2001**, *3*, 1121–1124.

(27) Uiterweerd, P. G. H.; van der Sluis, M.; Kaptein, B.; de Lange, B.; Kellogg, R. M.; Broxterman, Q. B. (S)-1-Aminoindane: Synthesis by Chirality Transfer Using (R)-Phenylglycine Amide as Chiral Auxiliary. *Tetrahedron: Asymmetry* **2003**, *14*, 3479–3485.

(28) Bruggink, A.; Roos, E. C.; de Vroom, E. Penicillin Acylase in the Industrial Production of β -Lactam Antibiotics. *Org. Process Res. Dev.* **1998**, *2*, 128–133.

- (29) Leeman, M. Resolutions of Racemates by Crystallization Additives and Attrition. PhD Thesis, University of Groningen, 2009; ISBN: 978-90-367-38422 (electronic version).
- (30) Roisnel, T.; Rodriguez-Carvajal, J. WinPLOTR: A Windows Tool for Powder Diffraction Pattern Analysis. *Mater. Sci. Forum* **2001**, 378–381, 118–123.
- (31) Rodriguez-Carvajal, J. FULLPROF: A Program for Rietveld Refinement and Pattern-Matching Analysis. *Abstr. Meet. Powder Diffraction, Toulouse, Fr.* **1990**, 127–128.
- (32) *Crys Alis PRO*; Rigaku Oxford Diffraction: Oxford, UK, 2018.
- (33) Sheldrick, G. M. SHELXT – Integrated Space-Group and Crystal-Structure Determination. *Acta Crystallogr., Sect. A: Found. Adv.* **2015**, 71, 3–8.
- (34) Sheldrick, G. M. Crystal Structure Refinement with SHELXL. *Acta Crystallogr., Sect. C: Struct. Chem.* **2015**, 71, 3–8.
- (35) Hübschle, C. B.; Sheldrick, G. M.; Dittrich, B. ShelXle: A Qt Graphical User Interface for SHELXL. *J. Appl. Crystallogr.* **2011**, 44, 1281–1284.
- (36) Dolomanov, O. V.; Bourhis, L. J.; Gildea, R. J.; Howard, J. a. K.; Puschmann, H. OLEX2: A Complete Structure Solution, Refinement and Analysis Program. *J. Appl. Crystallogr.* **2009**, 42, 339–341.
- (37) Macrae, C. F.; Bruno, I. J.; Chisholm, J. A.; Edgington, P. R.; McCabe, P.; Pidcock, E.; Rodriguez-Monge, L.; Taylor, R.; van de Streek, J.; Wood, P. A. Mercury CSD 2.0 – New Features for the Visualization and Investigation of Crystal Structures. *J. Appl. Crystallogr.* **2008**, 41, 466–470.
- (38) Allen, F. H.; Johnson, O.; Shields, G. P.; Smith, B. R.; Towler, M. CIF Applications. XV. EnCIFer: A Program for Viewing, Editing and Visualizing CIFs. *J. Appl. Crystallogr.* **2004**, 37, 335–338.
- (39) Dyadkin, V.; Pattison, P.; Dmitriev, V.; Chernyshov, D. IUCr. A New Multipurpose Diffractometer PILATUS@SNBL. *J. Synchrotron Radiat.* **2016**, 23, 825–829.
- (40) Hinrichsen, B.; Dinnebier, R. E.; Jansen, M. Datasqueeze: A Software Tool for Powder and Small-Angle X-Ray Diffraction Analysis. In *Commission on Powder Diffraction. Hrsq.: Int. Union of Crystallography Newsl.* **2005**, 12–22.
- (41) Favre-Nicolin, V.; Černý, R. FOX, 'free Objects for Crystallography': A Modular Approach to Ab Initio Structure Determination from Powder Diffraction. *J. Appl. Crystallogr.* **2002**, 35, 734–743.
- (42) Coelho, A. A. TOPAS-Academic; Coelho Software: Brisbane, 2012.
- (43) Evans, J. S. O. Advanced Input Files & Parametric Quantitative Analysis Using Topas. *Mater. Sci. Forum* **2010**, 651, 1–9.
- (44) Tumanova, N.; Tumanov, N.; Robeyns, K.; Fischer, F.; Fusaro, L.; Morelle, F.; Ban, V.; Hautier, G.; Filinchuk, Y.; Wouters, J.; Leyssens, T.; Emmerling, F. Opening Pandora's Box: Chirality, Polymorphism, and Stoichiometric Diversity in Flurbiprofen/Proline Cocrystals. *Cryst. Growth Des.* **2018**, 18, 954–961.
- (45) Tumanov, I. A.; Achkasov, A. F.; Boldyreva, E. V.; Boldyrev, V. V. Following the Products of Mechanochemical Synthesis Step by Step. *CrystEngComm* **2011**, 13, 2213–2216.
- (46) Linol, J.; Morelli, T.; Petit, M.-N.; Coquerel, G. Inversion of the Relative Stability between Two Polymorphic Forms of (±) Modafinil under Dry High-Energy Milling: Comparisons with Results Obtained under Wet High-Energy Milling. *Cryst. Growth Des.* **2007**, 7, 1608–1611.
- (47) Karki, S.; Friščić, T.; Jones, W. Control and Interconversion of Cocrystal Stoichiometry in Grinding: Stepwise Mechanism for the Formation of a Hydrogen-Bonded Cocrystal. *CrystEngComm* **2009**, 11, 470–481.
- (48) Fischer, F.; Lubjuhn, D.; Greiser, S.; Rademann, K.; Emmerling, F. Supply and Demand in the Ball Mill: Competitive Cocrystal Reactions. *Cryst. Growth Des.* **2016**, 16, 5843–5851.
- (49) Friščić, T.; Jones, W. Recent Advances in Understanding the Mechanism of Cocrystal Formation via Grinding. *Cryst. Growth Des.* **2009**, 9, 1621–1637.
- (50) Tumanova, N.; Tumanov, N.; Fischer, F.; Morelle, F.; Ban, V.; Robeyns, K.; Filinchuk, Y.; Wouters, J.; Emmerling, F.; Leyssens, T. Exploring Polymorphism and Stoichiometric Diversity in Naproxen/Proline Cocrystals. *CrystEngComm* **2018**, 20, 7308–7321.
- (51) Manoj, K.; Tamura, R.; Takahashi, H.; Tsue, H. Crystal Engineering of Homochiral Molecular Organization of Naproxen in Cocrystals and Their Thermal Phase Transformation Studies. *CrystEngComm* **2014**, 16, 5811–5819.
- (52) Lee, E. C.; McCauley, K. M.; Fu, G. C. Catalytic Asymmetric Synthesis of Tertiary Alkyl Chlorides. *Angew. Chem., Int. Ed.* **2007**, 46, 977–979.
- (53) Goj, O.; Kotila, S.; Haufe, G. Convenient Routes to 2-Aryl-2-Fluoropropionic Acids: Synthesis of Monofluorinated Analogues of (±)-Ibuprofen, (±)-Naproxen and Related Compounds. *Tetrahedron* **1996**, 52, 12761–12774.
- (54) Banti, C. N.; Papatriantafyllopoulou, C.; Tasiopoulos, A. J.; Hadjikakou, S. K. New Metalo-Therapeutics of NSAIDs against Human Breast Cancer Cells. *Eur. J. Med. Chem.* **2018**, 143, 1687–1701.
- (55) Batzdorf, L.; Fischer, F.; Wilke, M.; Wenzel, K.-J.; Emmerling, F. Direct In Situ Investigation of Milling Reactions Using Combined X-Ray Diffraction and Raman Spectroscopy. *Angew. Chem., Int. Ed.* **2015**, 54, 1799–1802.
- (56) Užarević, K.; Halasz, I.; Friščić, T. Real-Time and in Situ Monitoring of Mechanochemical Reactions: A New Playground for All Chemists. *J. Phys. Chem. Lett.* **2015**, 6, 4129–4140.
- (57) Springuel, G.; Robeyns, K.; Norberg, B.; Wouters, J.; Leyssens, T. Cocrystal Formation between Chiral Compounds: How Cocrystals Differ from Salts. *Cryst. Growth Des.* **2014**, 14, 3996–4004.